FEMS Microbiology Letters (Revised manuscript)

A novel *gnd* mutation leading to increased L-lysine production in *Corynebacterium glutamicum*

Junko Ohnishi [a], Ritsuko Katahira [a], Satoshi Mitsuhashi [a], Shingo Kakita [a], Masato Ikeda [b,*]

Keywords: *Corynebacterium glutamicum*; 6-phosphogluconate dehydrogenase; L-lysine

[a] *Tokyo Research Laboratories, Kyowa Hakko Kogyo Co., Ltd., Asahi-machi, Machida, Tokyo 194-8533, Japan*

[b] *Department of Bioscience and Biotechnology, Faculty of Agriculture, Shinshu University, Minami-minowa, Kami-ina, Nagano 399-4598, Japan*

*Corresponding author.

Masato Ikeda, Ph. D.

Present address: Department of Bioscience and Biotechnology, Faculty of Agriculture, Shinshu University, Minami-minowa, Kami-ina, Nagano 399-4598, Japan. Tel.: +81 (265) 77 1614; Fax: +81 (265) 77 1629.

E-mail address: m_ikeda@shinshu-u.ac.jp

Abstract

Toward more efficient L-lysine production, we have been challenging genome-based strain breeding by the approach of assembling only relevant mutations in a single wild-type background. Following the creation of a new L-lysine producer *Corynebacterium glutamicum* AHP-3 that carried three useful mutations (*lysC311*, *hom59*, and *pyc458*) on the relevant downstream pathways, we shifted our target to the pentose phosphate pathway. Comparative genomic analysis for the pathway between a classically derived L-lysine producer and its parental wild-type identified several mutations. Among these mutations, a Ser-361→Phe mutation in the 6-phosphogluconate dehydrogenase gene (*gnd*) was defined as a useful mutation for L-lysine production. Introduction of the *gnd* mutation into strain AHP-3 by allelic replacement led to approximately 15% increased L-lysine production. Enzymatic analysis revealed that the mutant enzyme was less sensitive than the wild-type enzyme to allosteric inhibition by intracellular metabolites, such as fructose 1,6-bisphosphate, D-glyceraldehyde 3-phosphate, phosphoribosyl pyrophosphate, ATP, and NADPH, which were known to inhibit this enzyme. Isotope-based metabolic flux analysis demonstrated that the *gnd* mutation resulted in 8% increased carbon flux through the pentose phosphate pathway during L-lysine production. These results indicate that the *gnd* mutation is responsible for diminished allosteric regulation and contributes to redirection of more carbon to the pentose phosphate pathway that was identified as the primary source for NADPH essential for L-lysine biosynthesis, thereby leading to improved product formation.

1. Introduction

Corynebacterium glutamicum and related bacteria are industrially important microorganisms that are widely used for the production of various amino acids [1,2]. Commercially potent amino acids producers of *C. glutamicum* have been developed mostly by repeated random mutation and selection [2,3,4]. While the classical mutagenic procedure has greatly contributed to the improvement of production yield, most of the useful genetic properties have lain idle within individual mutants and have not so far been actively exploited [1].

Our laboratories have recently determined the whole genome sequence of the representative wild-type strain of *C. glutamicum,* ATCC 13032 [1,5]. The availability of the genomic data facilitated our comparative genomic analysis of a classically derived industrial strain to decipher the results obtained by repeated random mutation selection. Following this, we have been conducting genome-based strain breeding, which involves identifying mutations by comparative genomic analysis, defining mutations beneficial for production, and assembling them in a single wild-type background [6]. As already demonstrated by the generation of an efficient L-lysine-producing *C. glutamicum* mutant AHP-3 that carried three beneficial mutations (*lysC311, hom59, pyc458*), the approach is useful not only for creating industrially more advantageous strains but also for rationalizing production mechanisms [6,7].

Toward the elucidation of advanced mechanisms of L-lysine production and further yield improvement, we have directed our attention from the downstream pathways to upstream central metabolism, especially the pentose phosphate pathway. The pentose phosphate pathway plays several key roles in metabolism, including the supply of reducing power and biosynthetic carbon skeletons. So far, relationships between L-lysine production and carbon flux through the pathway have been well documented for *C. glutamicum* in the light of the role in regenerating NADPH needed for L-lysine biosynthesis [8,9,10,11]. Metabolic flux analysis has indicated that the main site of NADPH generation during L-lysine production is the oxidative part of the pentose phosphate pathway in this microorganism [9]. It has

been also established that in *C. glutamicum* the production of L-lysine correlates with the extent of NADPH generation [8,9,11]. However, no mutation leading to increased L-lysine production has been reported with respect to the pentose phosphate pathway. In addition, there has been no example of metabolic engineering to redirect carbon through the pentose phosphate pathway except the works by Mascarenhas et al. [12] and Marx et al. [13]. They both described carbon redirection from glycolysis to the pentose phosphate pathway by disruption of the *pgi* gene encoding phosphoglucose isomerase, the first enzyme specific for glycolysis.

Our sequencing analysis of genes on the pentose phosphate pathway of a classically derived L-lysine-producing strain B-6 [14], followed by comparing the sequences with the corresponding wild-type sequences already available, revealed point mutations in the glucose 6-phosophate dehydrogenase gene (*zwf*), the 6-phosphogluconate dehydrogenase gene (*gnd*), the transaldolase gene (*tal*), and the transketolase gene (*tkt*). Among the four single base-pair mutations identified, the mutation found in *gnd* was shown to be relevant to L-lysine production. Here, focusing on the beneficial *gnd* mutation, we describe the enzymatic and metabolic consequences of the mutation in the newly developed L-lysine producer AHP-3.

2. Materials and methods

2.1. Bacterial strains and plasmids

The L-lysine-producing strain used for comparative genomic analysis is *C. glutamicum* B-6 [14] derived by multiple rounds of mutagenesis from a wild-type strain *C. glutamicum* ATCC 13032. This production strain has many mutations that lead to resistance to an L-lysine structural analog, *S*-(2-aminoethyl)-L-cysteine (AEC), rifampicin, streptomycin, and 6-azauracil. *C. glutamicum* AHP-3 [6], used as a host for evaluation of mutations on the pentose phosphate pathway of strain B-6, is a new L-lysine producer developed by a genome-based approach from the wild-type ATCC 13032. It carries only three mutations (*hom59*, *lysC311*, and *pyc458*) that are essential for high-level production of L-lysine. *E. coli* DH5α was used as a host for cloning of the PCR products. Plasmid pCgnd361 that contained

the mutant *gnd* gene in vector pESB30 [6] was used to replace the wild-type chromosomal gene by the mutant gene.

2.2. Media and culture conditions

Complete media BY [15] and BYG [16] were used for cultivation of the coryneform bacteria. Solid plates were made by the addition of Bacto-Agar (Difco) to 1.6%. When required, kanamycin was added at the final concentration of 20 μg ml^{-1} for BY plates. LPG2 medium used for L-lysine production in a 300-ml flask consisted of (per liter) 50 g of glucose, 10 g of corn steep liquor, 45 g of $(NH_4)_2SO_4$, 4.5 g of urea, 0.5 g of KH_2PO_4, 0.5 g of $MgSO_4 \cdot 7H_2O$, 10 mg of $FeSO_4 \cdot 7H_2O$, 10 mg of $MnSO_4 \cdot 4H_2O$, 5 mg of β-alanine, 5 mg of nicotinic acid, 5 mg of thiamine-HCl, 0.3 mg of D-biotin, and 30 g of $CaCO_3$ (pH 7.2). For an isotope-based metabolic flux analysis, LPG2 medium was modified as follows. The carbon source, 50g of glucose, was replaced by the mixture of 45 g of [1-^{13}C]glucose and 5 g of [U-$^{13}C_6$]glucose (99% enriched, ISOTEC, USA) per liter. In addition, a natural source, corn steep liquor, was excluded to minimize interferences of amino acids derived from the corn steep liquor in MS measurement and NMR analysis. A 3.0-ml sample of the seed culture grown to early stationary phase at 30°C in BYG medium was inoculated into 30 ml of LPG2 medium or modified LPG2 medium in a 300-ml flask. The culture was performed on a rotary shaker at 30°C. For growth of *E. coli*, LB medium [17] was used. Cell growth, glucose concentration, and L-lysine titer were measured as described previously [6]. L-lysine titer was determined as L-lysine HCl.

2.3. Recombinant DNA techniques

Standard protocol [17] was used for the construction, purification and analysis of plasmid DNA, and for transformation of *E. coli*. Chromosomal DNA was extracted from protoplasts of L-lysine producer B-6 by the method of Saito and Miura [18]. The protoplasts were prepared by the method of Katsumata et al. [15]. Transformation of *C. glutamicum* by electroporation was carried out by the method of van der Rest et al. [19], using Gene pulser and Pulse controller (BioRad, USA). PCR was performed with DNA Thermal Cycler GeneAmp 9600 (Perkin Elmer, USA), using *Taq* polymerase obtained from Boehringer Mannheim (Germany) for the

routine applications, or Pyrobest DNA polymerase (Takara, Japan), when high fidelity was required.

2.4. Identification of a mutation in gnd

The *gnd* gene was PCR amplified from genomic DNA of L-lysine producer B-6. PCR primer sequences were designed as follows, based on the nucleotide sequences of a region flanking the intact gene publicly available at http://gib.genes.nig.ac.jp/single/index.php?spid=Cglu_ATCC13032 (ORF name; Cgl1452).

gnd -F: 5'-CACCGGGCTATGCCGTCAAGTAC-3'

gnd -R: 5'-TTAAGCTTCAACCTCGGAGCGGT-3'

The PCR product was cloned into vector pESB30 to yield plasmid pCgnd361 by the TA cloning method as described previously [6]. The nucleotide sequence of the cloned *gnd* gene was then analyzed and compared with the wild-type sequence already available.

2.5. Generation of defined mutant APG-4

The *gnd* mutation, S361F, on pCgnd361 was introduced into a new L-lysine producer AHP-3 (*hom59*, *lysC311*, *pyc458*) via two recombination events as described previously [6]. A strain carrying the *gnd* mutation was designated APG-4.

2.6. Enzyme assays

Cells were grown at 30°C in 30ml of LPG2 medium, harvested in mid-log-phase, washed with cold 50mM Tris-HCl buffer (pH 7.5), and suspended in 5ml of the same buffer. Cell disruption was achieved by sonication(model UR-200P; Tomy Seiko Co., Ltd.), and cell debris were removed by centrifugation at 8,000 x *g* for 15 min at 4°C. The supernatant was stored on ice until further use. The quantity of protein was determined by the method of Bradford [20]. Activities of 6-phosphogluconate dehydrogenase and glucose 6-phosphate dehydrogenase in crude cell extracts were measured spectrophotometrically at 30°C by determining the increase in the A340 of NADPH, essentially by the method of Sugimoto and Shiio [21].

2.7. Sample preparation for MS measurements and NMR analysis

Cells of strains AHP-3 and APG-4 were grown in modified LPG2 medium

without corn steep liquor until depletion of glucose, which was checked by analysis described above. The cells were chilled on ice and centrifuged at 4,000 x *g* for 10 min at 4°C to separate cells from the supernatant. The supernatants (the cell-free medium) were used directly for amino acid analysis. The cells were immediately washed with ice-cold deionized water, and stored at –70°C. After lyophilization, freeze-dried cells were then suspended in 6 N HCl and hydrolyzed at 110°C under N_2 atmosphere for 12 h as described by Marx et al. [22]. The hydrolysate was evaporated to dryness. After the addition of 15 ml of water, 2 ml of hydrolysate was used for MS measurement, and the residual was used for NMR analysis.

2.8. MS measurement

LC-MS spectra were recorded on Waters ZMD mass spectrometer (Micromass, Manchester, UK). The hydrolysate was filtrated by 0.45 µm filter. A 2 µl of filtrate was injected onto Waters Atlantis column ($C_{18,}$ 2.1 mm x 50 mm, 3.5 µm bead diameter) at a flow rate of 0.2 ml min^{-1}, and the isocratic gradient of 10% acetonitrile/90% H_2O was employed.

2.9. NMR analysis

The hydrolysate was evaporated again and redissolved in 0.5 ml of D_2O. NMR spectra were recorded at 500.13 MHz for ^1H and at 125.76 MHz for ^{13}C on Bruker DMX 500 spectrometer (Bruker Biospin, Karlsruhe, Germany) at 20°C. Heteronuclear single-quantum correlated (HSQC) spectra in States-mode were recorded [23]. HSQC spectra were collected with 512 complex points in t_1 and 2048 complex points in the t_2 dimension. The t_2 FIDs were multiplied by a shifted sine-bell square window function and then Fourier transformed. The t_1 data were apodized with the same window function, zero-filled to 2048 complex points, and then Fourier transformed. Assignments of the ^{13}C and ^1H signals of amino acids were carried out by comparing their chemical shifts with published data [24]. ^{13}C isotopomer distributions in amino acids were determined from ^{13}C spectra and J-scaling HSQC [25]. ^{13}C spectra were acquired under continuous composite pulse broadband decoupling using 30^o pulse, a sweep width of 6 kHz, and a repetition time of 2 s. J-scaling HSQC spectra with a scaling factor of 8 were collected with 1024

complex points in t_1 and 4096 complex points in t_2. Other procedures were the same as HSQC spectra. Since the values of fractional enrichments obtained from DQF-COSY spectra were fluctuated depending on the processing parameters such as window function or data size, we measured these values from the isolated peaks in 1D spectrum. All the data processings were carried out using the program XWINNMR (Bruker).

2.10. Metabolic flux analysis

For the estimation of intracellular metabolic fluxes, we introduced a mathematical model programmed in MATLAB 6.5 and SIMULINK 4.1 [26-30]. This model was further extended and modified to obtain the intracellular fluxes using intensity ratios of ^{13}C and MS isotopomers in addition to fractional enrichments. All the calculations were performed on a personal computer. The biochemical network of the *C. glutamicum* metabolism comprising 37 different fluxes was shown in Fig. A1. In total, 37 different fluxes were determined through 28 experimental constraints resulted from 11 stoichiometric balances described in appendix, 7 stoichiometric measurements (trehalose, lactate, pyruvate, acetate, L-alanine, L-valine, and L-lysine), and 10 estimated fluxes to biomass. Additional constraints were obtained from ^{13}C labeling data. The network was overdetermined by the measurement of intensity ratios of mass isotopomer to estimate 9 flux parameters. The definition of these flux parameters is given in the appendix. Nonlinear mapping of the exchange fluxes v^{exch} on exchange coefficients $v^{exch[0,1]}$, given by the following equation: $v^{exch} = v^{exch[0,1]} \times \beta / (1-v^{exch[0,1]})$, was applied to overcome the numerical problems arising from very large parameter values [28]. Here, β is a constant on the order of magnitude of the occurring net fluxes. A value of $\beta = 1$ was used in this study. As reported by Yang et al. [31], the exchange coefficients defined below were limited to values below 0.95, because large exchange rates affect the speed of convergence so that the presence of several highly reversible reactions results in a significantly higher computational effort. The flux estimation was based on the optimization function 'fminsearch' implemented in MATLAB. The flux was estimated by minimization of the sum of the squares of the relative deviations between

experimental and modeled intensity ratios of ^{13}C and MS isotopomers as well as fractional enrichments. For the estimation of 95% confidence region of the flux parameters, synthetic measurement data were generated by the addition of normally distributed measurement noise to simulated measurement data. For MS data, the standard deviation in the measurement data was assessed from multiple measurements. For NMR data, it was estimated from the noise level. Then the flux parameter estimation routines were started from 50 synthetic data sets, and 95% confidence region of the parameters was estimated from the results.

3. Results

3.1. Identification of a point mutation in 6-phosphogluconate dehydrogenase

The *gnd* gene, covering each putative promoter and terminator regions, was isolated from genomic DNA of a classically derived L-lysine-producing mutant B-6 by PCR, and the nucleotide sequence was determined. The sequence was compared with the corresponding wild-type sequence, revealing a point mutation: a T to C exchange at position 1083, leading to an amino acid replacement of Ser-361 by Phe. To speculate on the function of Ser at position 361, the predicted amino acid sequence was aligned with the 6-phosphogluconate dehydrogenase sequences of other origins *Escherichia coli*, *Mycobacterium tubercurosis*, the cyanobacterium *Synechococcus* sp. PCC7942, and *Lactococcus lactis*. Although amino acid residues responsible for substrate binding and coenzyme binding [32] are conserved in *C. glutamicum*, the Ser residue at position 361 is located outside of those motifs. However, it was found that residues corresponding to position 361 of *C. glutamicum* are fully conserved in those organisms (data not shown). From these findings, it was suggested that the residue might not be related directly to the binding of the substrate or coenzyme, but might affect other enzymatic properties such as allosteric regulation.

3.2. Introduction and evaluation of the gnd mutation

The *gnd* mutation (S361F, designated *gnd361*) was introduced into the new L-lysine production strain AHP-3 (*lysC311, hom59, pyc458*) by allelic replacement

using plasmid pCgnd361, resulting in the creation of tetra-mutation strain APG-4. Comparative phenotypic analysis showed no distinct differences between strains AHP-3 and APG-4 with respect to the drug-resistant phenotypes used as selection markers for isolation of the classical L-lysine producer B-6 from the wild type strain ATCC 13032 (see Materials & Methods), indicating that the *gnd361* mutation was not related to any drug resistance in strain B-6. L-lysine production by strain APG-4 was then investigated using a flask. As shown in Fig. 1, strain APG-4 showed almost the same growth rate as the parental strain, AHP-3, and accumulated approximately 15% higher L-lysine compared to strain AHP-3, indicating that the *gnd361* mutation was relevant to L-lysine production. No distinct differences in sugar consumption rate were observed between the two strains, thus leading to completion of fermentation around 33 h. Five separate cultures showed that the effect was highly reproducible and statistically significant.

3.3. Characterization of wild-type and mutant enzymes

To elucidate underlying mechanism for the increased production by strain APG-4, the mutant 6-phosphogluconate dehydrogenase was analyzed in comparison with the wild-type enzyme using crude cell extracts. The specific activity of the mutant enzyme was near 60% lower than the wild-type enzyme (Table 1). On the other hand, when glucose 6-phosphate dehydrogenase, the other key enzyme in the pentose phosphate pathway, was measured as an internal control, significant differences were not observed between these two strains (Table 1). We next examined how the mutation influenced the allosteric properties of the enzyme since 6-phosphogluconate dehydrogenase of *C. glutamicum* is known to be allosterically regulated by several metabolites such as fructose 1,6-bisphosphate, D-glyceraldehyde 3-phosphate, phosphoribosyl pyrophosphate, ATP, and NADPH [21,33]. When the wild-type enzyme was examined for its activity in the presence of each effector around the intracellular concentration reported in this bacterium [33,34,35], the activity was indeed reduced as reported in the literature [21,33]. In contrast, the mutant enzyme was found to be less sensitive to all effectors tested here (Table 2), revealing that the *gnd361* mutation was responsible for diminished

allosteric regulation.

3.4. Metabolic flux response to introduction of gnd361 mutation

To investigate how the *gnd361* mutation influences the carbon flux through the pentose phosphate pathway during L-lysine production, strains AHP-3 and APG-4 were subjected to ^{13}C glucose-labeling experiments in shake flask fermentation combined with metabolite balancing. Cultures were conducted with modified LPG2 medium without a natural material, corn steep liquor, to minimize interferences of extracellulary supplied amino acids in both MS measurement and NMR analysis. Under the suboptimal conditions, L-lysine production of both strains was somewhat decreased as compared with that of the optimal conditions shown in Fig. 1 and, in addition, the difference of L-lysine production between strains AHP-3 and APG-4 was relatively small. However, we confirmed the reproducibility of the difference through five separate cultures. The profiles of growth and product formation were basically similar to those of flask cultivation as shown in Fig. 1. The estimation of intracellular flux distribution was carried out for each strain by minimizing the deviation between experimental and calculated data as shown in Tables 3, 4, and 5. The best-fit flux distribution of two strains is given in Fig. 2. Although substantial changes were not observed in overall pathway fluxes, the pentose phosphate pathway flux of 38% and 41% was estimated for the parent strain and the *gnd* mutant, respectively, i.e., about 8% enhanced flux in response to the introduction of the *gnd361* mutation. The estimation of 95% confidence region of the flux parameters indicated that the estimated increase in carbon flow through the pathway was statistically significant. Meanwhile the flux through the TCA cycle decreased slightly in strain APG-4 as compared with strain AHP-3, probably as a consequence of increased carbon flow into the L-lysine-biosynthetic pathway.

4. Discussion

The allosteric enzyme 6-phosphogluconate dehydrogenase, along with glucose 6-phosophate dehydrogenase, is regarded as the rate-controlling enzyme of the pentose phosphate pathway in *C. glutamicum* [21,33]. While the importance of the

enzyme for the pathway flux has been previously described [8,9,11], this is the first report on a *gnd* mutation that leads to increased carbon flux in the pathway. Enzymatic and metabolic flux analyses, performed with a mutant derived from strain AHP-3 and bearing the Ser361Phe mutation, were consistent with the hypothesis that this mutation alleviated the allosteric regulation of the enzyme and caused an 8% increase in carbon flux through the pathway. These observations thus promote the view that the mutation-derived alleviation of the enzyme from allosteric regulation contributes to redirection of more carbon to the pentose phosphate pathway although the mutation concomitantly caused a decrease in the specific enzyme activity. Considering the previous work indicating that the pentose phosphate pathway in *C. glutamicum* was primarily regulated by the NADPH concentrations (33), the enhanced carbon flow through the pathway in strain APG-4 might be mainly attributed to the partial desensitization of the enzyme to NADPH rather than other allosteric effectors.

From the viewpoint of NADPH supply, it is of significance to grasp the fluxes within the pentose phosphate pathway and the TCA cycle because the glucose 6-phosphate dehydrogenase, the 6-phosphogluconate dehydrogenase, and the isocitrate dehydrogenase are the main NADPH sources of this organism [11,35]. Thus we focused on these pathways to approximate the total NADPH supply in the parent strain AHP-3 and its *gnd* mutant APG-4. As revealed by metabolic flux analysis (Fig. 2), the pentose phosphate pathway flux was 38.2% and 41.4% or the TCA cycle flux was 75.6% and 72.5% for strains AHP-3 and APG-4, respectively. This resulted in the NADPH formation per 1 mol glucose by the pentose phosphate pathway of 0.764 mol and 0.828 mol, or by the TCA cycle of 0.756 mol and 0.725 mol in strains AHP-3 and APG-4, respectively. It followed that the NADPH supply was estimated 1.520 mol and 1.553 mol in total in strains AHP-3 and APG-4, respectively, i.e., 0.033 mol higher NADPH regeneration in strain APG-4 than that in strain AHP-3. On the other hand, 1 mol L-lysine requires 4 mol NADPH for its biosynthesis from glucose [35]. Considering this, the NADPH demand for L-lysine synthesis was calculated 0.780 and 0.812 mol per 1 mol glucose, respectively, under

the cultivation conditions for the metabolic flux analysis shown in Fig. 2. The calculated increase (0.032 mol) in NADPH demand agreed fairly with the estimated increase (0.033 mol) in NADPH formation. This agreement could allow us to explain that increased availability of NADPH accelerated the NADPH-dependent enzymatic reactions relevant to L-lysine biosynthesis, thus leading to increased L-lysine production. Although the increase in L-lysine production is not large, it should be noted that even a small effect has a great impact on the economy of the commercial manufacture of the very large-scale bulk amino acid.

The *gnd361* mutation gave rise to a 15% increase in L-lysine production, provided that the cultivation was carried out under the optimal conditions (Fig. 1). Nevertheless, the contribution to production was small compared with the cases of other positive mutations already identified on the relevant terminal pathways [6]. One probable reason can be the incomplete deregulation of the mutant enzyme. If so, higher deregulation of the enzyme might lead to larger effect on L-lysine production. However, we should note that previous attempts to drastically redirect carbon flux into the pentose phosphate pathway resulted in growth impairment in *Corynebacterium* strains [13,36]. Considering this, the *gnd361* mutation that caused partial desensitization of the enzyme to allosteric inhibition, thereby leading to relatively small effect on carbon flow, might be rather adequate for an industrial use because genetic modifications resulting in growth impairment are practically undesirable. We are currently examining whether the substitution to other amino acids than phenylalanine at position Ser-361 is more useful or not in the light of not only a positive effect on production but also its physiological consequences.

As another reason for relatively small effect of the *gnd361* mutation on L-lysine production, it is likely that the other allosteric enzyme, glucose 6-phosphate dehydrogenase, would have now become the rate-limiting step in the pentose phosphate pathway because the enzyme remains to be wild type in strain APG-4. This possibility can be addressed by examining the effect of deregulation of the enzyme on L-lysine production. However, in microorganisms, mutations leading to desensitization of the enzyme to allosteric regulation, as well as their selectable

phenotype, have not been reported as far as we know. In this sence, it is worth attempting to search such mutations extensively from classically derived amino acids producers.

It is interesting to note that the single amino acid substitution of the *gnd* product resulted in simultaneous alleviation from allosteric inhibitions by all effectors examined here. Although there are no other examples of such mutant enzymes in bacterial 6-phosphogluconate dehydrogenase, Meyer et al. reported a similar mutation in an *Escherichia coli* allosteric enzyme, ADP-glucose pyrophosphorylase [37], in which site-directed mutagenesis was used to obtain the single mutation causing alteration of allosteric properties. In this case, the observation was interpreted by the allosteric model of Monod et al. [38]. Similarly in our case, the *gnd361* mutation might be involved in the conformational change of the enzyme, while at present we cannot explain the reason for the concomitant decrease of the specific activity observed in the mutant strain. Future studies on the allosteric sites of this enzyme and on the structure-function relationships in the presence and absence of the mutation will clarify the underlying mechanism.

Until this work, it has been almost impossible to purposely find a beneficial *gnd* mutation due to no known selectable phenotype. However, once such a mutation is obtained, it becomes possible to share the beneficial genetic property with other strains to be engineered. In this sence, the availability of the *gnd361* mutation will provide useful addition to the future metabolic engineering for improved production. Considering that the pentose phosphate pathway is responsible for supplying not only NADPH but also two important precursors for amino acid biosynthesis, ribose 5-phosphate and erythrose 4-phosphate required for L-histidine and aromatic biosynthesis, respectively, the newly identified *gnd* mutation can be expected to further improve existing *C. glutamicum* production strains of those amino acids.

Appendix

The following 11 balance equations of intracellular metabolites are formulated for the examined network applying the numbering of the fluxes of Fig. A1.

Glucose 6-phosphate: $v_1 - v_2 - v_3 - v_4 - v_5 + v_6 = 0$

Fructose 6-phosphate: $v_5 - v_6 - v_7 - v_8 + v_{11} - v_{12} + v_{15} - v_{16} = 0$

Pentose phosphate: $v_3 - v_9 - v_{11} + v_{12} - 2v_{13} + 2v_{14} = 0$

Erythrose 4-phosphate: $- v_{10} - v_{11} + v_{12} + v_{15} - v_{16} = 0$

Sedoheptulose 7-phosphate: $v_{13} - v_{14} - v_{15} + v_{16} = 0$

Glyceraldehyde 3-phosphate:

$2v_8 + v_{11} - v_{12} + v_{13} - v_{14} - v_{15} + v_{16} - v_{24} + v_{19} - v_{17} - v_{18} = 0$

Pyruvate: $v_{17} - v_{20} - v_{21} - v_{22} - 2v_{23} - v_{25} - v_{26} - v_{29} + v_{30} - v_{35} - v_{19} = 0$

Acetyl Co-A: $v_{26} - v_{27} - v_{28} - v_{31} = 0$

α-Ketoglutarate: $v_{31} - v_{32} - v_{33} = 0$

Oxaloacetate: $v_{29} - v_{30} - v_{31} + v_{33} - v_{34} - v_{35} = 0$

Δ-PDC: $v_{35} - v_{36} - v_{37} = 0$

Flux-partitioning ratios (Φ), and reversibilities (ζ) were defined as relative fluxes into one of the two branches, and as ratio of backward or exchange flux to the net flux in the forward direction, respectively. Flux parameters used here are the flux-partitioning ratio between glycolysis and the pentose phosphate pathway (Φ_{PPP}), the ratio between the alternative pathways in the lysine biosynthesis (Φ_{DH}), the ratio at the pyruvate node (Φ_{PC}), the reversibility of glucose 6-phosphate isomerase (ζ_{PGI}), the reversibility of transketolase (ζ_{TK1}, ζ_{TK2}), the reversibility of transaldolase (ζ_{TA}), the reversibility of fluxes between C4 metabolites of the TCA cycle, C3 metabolites from glycolysis ($\zeta_{PC/PEPCK}$), and the reversibility of enolase (ζ_{ENO}). These are defined as follows, applying the numbering of the fluxes of Fig. A1.

$\Phi_{PPP} = v_3 / (v_3 + v_5 - v_6)$

$\Phi_{PC} = (v_{29} - v_{30}) / (v_{26} + v_{29} - v_{30}) = (v_{32} + v_{34}) / (v_{26} + v_{32} + v_{34})$

$\Phi_{DH} = v_{36} / v_{35}$

$\zeta_{PC/PEPCK} = v_{30} / v_{29}$

$\zeta_{PGI} = v_6 / v_5$

$\zeta_{TA} = v_{16} / v_{15}$

$\zeta_{TK1} = v_{12} / v_{11}$

$\zeta_{TK2} = v_{14} / v_{13}$

$\zeta_{ENO} = v_{19} / v_{17}$

Acknowledgments

The authors thank Dr. C. Wittmann for supplying the mathematical tools for fractional ^{13}C-labeling analysis. The authors appreciate discussions with T. Nakano, M. Maeda, M. Hayashi, K. Tanaka, H. Mizoguchi, T. Abe, Y. Yonetani, M. Yagasaki, S. Hashimoto, K. Ochiai, and S. Koizumi.

References

[1] Ikeda, M. and Nakagawa, S. (2003) The *Corynebacterium glutamicum* genome: features and impacts on biotechnological process. Appl. Microbiol. Biotechnol. 62, 99-109.

[2] Kinoshita, S. and Nakayama, K. (1978) Amino acids. pp. 209-261. *In* A. H. Rose (ed.), Primary products of metabolism. Academic press, London, England.

[3] Demain, A. L. (2000) Microbial biotechnology. Trends Biotechnol. 18, 26-31.

[4] Ikeda, M. (2003) Amino acid production process. Adv. Biochem. Eng. Biotechnol. 79, 1-35.

[5] Nakagawa, S., Mizoguchi, H., Ando, S., Hayashi, M., Ochiai, K., Yokoi, H., Tateishi, N., Senoh, A., Ikeda, M. and Ozaki, A. (2001) Novel polynucleotides. European patent 1,108,790.

[6] Ohnishi, J., Mitsuhashi, S., Hayashi, M., Ando, S., Yokoi, H., Ochiai, K. and Ikeda, M. (2002) A novel methodology employing *Corynebacterium glutamicum* genome information to generate a new L-lysine-producing mutant. Appl. Microbiol. Biotechnol. 58, 217-223.

[7] Ohnishi, J., Hayashi, M., Mitsuhashi, S. and Ikeda, M. (2003) Efficient 40°C fermentation of L-lysine by a new *Corynebacterium glutamicum* mutant developed by genome breeding. Appl. Microbiol. Biotechnol. 62, 69-75.

[8] Ishino, S., Shimomura-Nishimuta, J., Yamaguchi, K., Shirahata, K. and Araki, K. (1991) ^{13}C Nuclear magnetic resonance studies of glucose metabolism in L-glutamic acid and L-lysine fermentation by *Corynebacterium glutamicum*. J. Gen. Appl.

Microbiol. 37, 157-165.

[9] Marx, A., Striegel, K., de Graaf, A. A., Sahm, H. and Eggeling, L. (1997) Response of the central metabolism of *Corynebacterium glutamicum* to different flux burdens. Biotechnol. Bioeng. 56,168-180.

[10] Vallino, J. J. and Stephanopoulos, G. (1994) Carbon flux distributions at the glucose 6-phosphate branch point in *Corynebacterium glutamicum* during lysine overproduction. Biotechnol. Prog. 10, 327-334.

[11] Wittmann, C. and Heinzle, E. (2002) Genealogy profiling through strain improvement by using metabolic network analysis: metabolic flux genealogy of several generations of lysine-producing Corynebacteria. Appl. Environ. Microbiol. 68, 5843-5859.

[12] Mascarenhas, D., Ashworth, D. J. and Chen, C. S. (1991) Deletion of *pgi* alters tryptophan biosynthesis in a genetically engineered strain of *Escherichia coli*. Appl. Environ. Microbiol. 57, 2995-2999.

[13] Marx, A., Hans, S., Möckel, B., Bathe, B. and de Graaf, A. A. (2003) Metabolic phenotype of phosphoglucose isomerase mutants of *Corynebacterium glutamicum*. J. Biotechnol. 104,185-197.

[14] Hirao, T., Nakano, T., Azuma, T., Sugimoto, M. and Nakanishi, T. (1989) L-lysine production in continuous culture of an L-lysine hyperproducing mutant of *Corynebacterium glutamicum.* Appl. Microbiol. Biotechnol. 32, 269-273.

[15] Katsumata, R., Ozaki, A., Oka, T. and Furuya, A. (1984) Protoplast transformation of glutamate-producing bacteria with plasmid DNA. J. Bacteriol. 159, 306-311.

[16] Ikeda, M. and Katsumata, R. (1999) Hyperproduction of tryptophan by *Corynebacterium glutamicum* with the modified pentose phosphate pathway. Appl. Environ. Microbiol. 65, 2497-2502.

[17] Sambrook, J. and Russell, D. W. (2001) Molecular cloning: a laboratory manual, 3rd ed. Cold Spring Harbor Laboratory Press, Cold Spring Harbor, N. Y.

[18] Saito, H. and Miura, K. (1963) Preparation of transforming deoxyribonucleic acid by phenol treatment. Biochim. Biophys. Acta 72, 619-629.

[19] van der Rest, M. E., Lange, C. and Molenaar, D. (1999) A heat shock following electroporation of *Corynebacterium glutamicum* with xenogeneic plasmid DNA. Appl. Microbiol. Biotech. 52, 541-545.

[20] Bradford, M. M. (1976) A rapid and sensitive method for the quantitation of microgram quantities of protein utilizing the principle of protein-dye binding. Anal. Biochem. 72, 248-254.

[21] Sugimoto, S. and Shiio, I. (1987) Regulation of 6-phosphogluconate dehydrogenase in *Brevibacterium flavum*. Agric. Biol. Chem. 51, 1257-1263.

[22] Marx, A., de Graaf, A. A., Wiechert, W., Eggeling, L. and Sahm, H. (1996) Determination of the fluxes in the central metabolism of *Corynebacterium glutamicum* by nuclear magnetic resonance spectroscopy combined with metabolite balancing. Biotechnol. Bioeng. 49, 111-129.

[23] Kay, L. E., Keifer, P. and Saarinen, T. (1992) Pure absorption gradient enhanced heteronuclear single quantum correlation spectroscopy with improved sensitivity. J. Am. Chem. Soc. 114, 10663-10665.

[24] Wüthrich, K. (1986) NMR of Proteins and Nucleic Acids. John Wiley & Sons, Inc., New York, N. Y.

[25] Willker, W., Flögel, U. and Leibfritz, D. (1997) Ultra-high-resolved HSQC spectra of multiple-^{13}C-labeled biofluids. J. Magn. Reson. 125, 216-219.

[26] Schmidt, K., Carlsen, M., Nielsen, J. and Villadsen, J. (1997) Modeling isotopomer distributions in biochemical networks using isotopomer mapping matrices. Biotechnol. Bioeng. 55, 831-840.

[27] Schmidt, K., Nielsen, J. and Villadsen, J. (1999) Quantitative analysis of metabolic fluxes in *Escherichia coli*, using two-dimensional NMR spectroscopy and complete isotopomer models. J. Biotechnol. 71, 175-190.

[28] Schmidt, K. and Nørregaard, L.C. (1999) Quantification of intracellular metabolic fluxes from fractional enrichment and ^{13}C–^{13}C coupling constraints on the isotopomer distribution in labeled biomass components. Metabol. Eng. 1, 166-179.

[29] Wittmann, C. and Heinzle, E. (1999) Mass spectrometry for metabolic flux analysis. Biotechnol. Bioeng. 62, 739-750.

[30] Wittmann, C. and Heinzle, E. (2001) Application of MALDI-TOF MS to lysine-producing *Corynebacterium glutamicum*. A novel approach for metabolic flux analysis. Eur. J. Biochem. 268, 2441-2455.

[31] Yang, C., Hua, Q. and Shimizu, K. (2002) Quantitative analysis of intracellular metabolic fluxes using GC-MS and two-dimensional NMR spectroscopy. J. Biosci. Bioeng. 93, 78-87.

[32] Tetaud, E., Hanau, S., Wells, J. M., Page, R. W. F., Adams, M. J., Arkison, S. and Barrett, M. P. (1999) 6-Phosphogluconate dehydrogenase from *Lactococcus lactis*: a role for arginine residues in binding substrate and coenzyme. Biochem. J. 338, 55-60.

[33] Moritz, B., Striegel, K., de Graaf, A. A. and Sahm, H. (2000) Kinetic properties of the glucose 6-phosphate and 6-phosphogluconate dehydrogenases from *Corynebacterium glutamicum* and their application for predicting pentose phosphate pathway flux *in vivo*. Eur. J. Biochem. 267, 3442-3452.

[34] Dominguez, H., Rollin, C., Guyonvarch, A., Guerquin-Kern, J. L., Cocaign-Bousquet, M. and Lindley, N. D. (1998) Carbon-flux distribution in the central metabolic pathways of *Corynebacterium glutamicum* during growth on fructose. Eur. J. Biochem. 254, 96-102.

[35] Moritz, B., Striegel, K., de Graaf, A. A. and Sahm, H. (2002) Changes of pentose phosphate pathway flux *in vivo* in *Corynebacterium glutamicum* during leucine-limited batch cultivation as determined from intracellular metabolite concentration measurements. Metabol. Eng. 4, 295-305.

[36] Kamada, N., Yasuhara, A., Takano, Y., Nakano, T. and Ikeda, M. (2001) Effect of transketolase modifications on carbon flow to the purine-nucleotide pathway in *Corynebacterium ammoniagenes*. 56, 710-717.

[37] Meyer, C. R., Bork, J. A., Nadler, S., Yirsa, J. and Preiss, J. (1998) Site-directed mutagenesis of a regulatory site of *Escherichia coli* ADP-glucose phosphorylase: the role of residue 336 in allosteric behavior. Arch. Biochem. Biophys. 353, 152-159.

[38] Monod, J., Wyman, J. and Changeux, J. P. (1965) On the nature of allosteric transitions: a plausible model. J. Mol. Biol. 12, 88-118.

Table 1

Activities of the key enzymes of the pentose phosphate pathway in strains AHP-3 and APG-4

	Specific activity (U mg^{-1})[a]	
Strain (genotype)	GND[b]	ZWF[b]
AHP-3 (*lysC311, hom59, pyc458*)	76	51
APG-4 (*lysC311, hom59, pyc458, gnd361*)	33	50

[a]One unit of the enzyme activity was defined as the amount catalyzing the formation of 1 nmol of NADPH per min. Results are the mean values of three measurements.

[b]GND, 6-phosphogluconate dehydrogenase; ZWF, glucose 6-phosphate dehydrogenase.

Table 2

Regulations of 6-phosphogluconate dehydrogenases by metabolites in strains AHP-3 and APG-4

Metabolite	Concentration (mM)	Relative activity (%)[a]	
		AHP-3	APG-4
None	-	100	100
FBP[b]	1	72	91
	3	60	86
G3P[b]	1	63	98
	3	20	85
PRPP[b]	1	84	96
	3	81	95
ATP	1	78	100
	3	54	65
NADPH	0.1	44	63
	0.3	16	26

[a]Relative to the activity without metabolites. Results are the mean values of three measurements.

[b]FBP, fructose 1,6-bisphosphate; G3P, D-glyceraldehyde 3-phosphate; PRPP, phosphoribosyl pyrophosphate.

Table 3

MS isotopomer intensity ratios of amino acids from strains AHP-3 and APG-4[a]

	AHP-3		APG-4	
Amino acid[b]	Exp m/m + 1	Calc m/m + 1	Exp m/m + 1	Calc m/m + 1
L-Lysine	0.63	0.63	0.65	0.65
L-Alanine	1.71	1.74	1.77	1.77

[a]Experimental data (Exp) obtained by MS measurements and calculated values (Calc) predicted by the solution of the mathematical model corresponding to the optimized set of fluxes.

[b]Experimental data of L-lysine and L-alanine were obtained by LC-MS. Results are the mean values of three measurements.

Table 4

^{13}C enrichments in carbon atoms of L-lysine and trehalose from strains AHP-3 and APG-4[a]

Analyte	Carbon position	^{13}C enrichment (%)			
		AHP-3		APG-4	
		Exp	Calc	Exp	Calc
L-Lysine	C-6	0.147	0.144	0.145	0.142
Trehalose	C-1	0.752	0.759	0.751	0.744

[a]Experimental data (Exp) obtained by NMR analysis and calculated values (Calc) predicted by the solution of the mathematical model corresponding to the optimized set of fluxes. Experimental data are the mean values of three measurements.

Table 5

Intensities of ^{13}C multiplet components as determined by 2D NMR spectra of cellular amino acids from strains AHP-3 and APG-4[a]

Carbon position	AHP-3								APG-4							
	Exp				Calc				Exp				Calc			
	s	*d1*	*d2*	*dd*	*s*	*d1*	*d2*	*dd*	*s*	*d1*	*d2*	*dd*	*s*	*d1*	*d2*	*dd*
Gly: α	0.36	0.64	-	-	0.35	0.65	-	-	0.38	0.62	-	-	0.36	0.64	-	-
Ser: α	0.17	0.09	0.14	0.60	0.17	0.05	0.18	0.60	0.16	0.09	0.17	0.58	0.20	0.10	0.16	0.58
Ser: β	0.76	-	0.24	-	0.77	-	0.23	-	0.76	-	0.24	-	0.77	-	0.23	-
Ala: α	0.22	0.07	0.16	0.55	0.20	0.08	0.18	0.54	0.27	0.07	0.15	0.51	0.21	0.06	0.22	0.51
Ala: β	0.76	-	0.24	-	0.76	-	0.24	-	0.76	-	0.24	-	0.76	-	0.24	-
Asp: α	0.46	0.16	0.20	0.18	0.43	0.17	0.20	0.20	0.49	0.16	0.20	0.15	0.43	0.17	0.20	0.20
Asp: β	0.57	0.18	0.17	0.08	0.56	0.18	0.19	0.07	0.57	0.18	0.17	0.08	0.56	0.18	0.19	0.07
Thr: γ	0.63	-	0.37	-	0.62	-	0.38	-	0.63	-	0.37	-	0.62	-	0.38	-
Pro: α	0.57	0.17	0.20	0.06	0.57	0.18	0.19	0.06	0.57	0.17	0.20	0.06	0.57	0.18	0.19	0.06
Pro: β	0.32	-	0.47	0.21	0.37	-	0.48	0.15	0.32	-	0.47	0.21	0.37	-	0.48	0.15
Pro: γ	0.57	-	0.35	0.08	0.60	-	0.35	0.05	0.57	-	0.35	0.08	0.60	-	0.35	0.05
Pro: δ	0.29	-	0.71	-	0.28	-	0.72	-	0.29	-	0.71	-	0.28	-	0.72	-
Lys: α	0.41	0.15	0.20	0.24	0.41	0.15	0.20	0.24	0.41	0.15	0.20	0.24	0.41	0.15	0.20	0.24
Lys: β	0.59	-	0.33	0.08	0.58	-	0.36	0.06	0.59	-	0.33	0.08	0.38	-	0.47	0.15
Lys: γ	0.35	-	0.49	0.16	0.37	-	0.48	0.15	0.35	-	0.49	0.16	0.38	-	0.47	0.15
Lys: δ	0.61	-	0.35	0.04	0.59	-	0.35	0.06	0.61	-	0.35	0.04	0.59	-	0.35	0.06
Lys: ε	0.38	-	0.62	-	0.37	-	0.63	-	0.38	-	0.62	-	0.37	-	0.63	-

[a] Experimental data (Exp) obtained by 2D NMR analysis and calculated values (Calc) predicted by the solution of the mathematical model corresponding to the optimized set of fluxes.

Figure legends

Fig. 1. L-lysine fermentation by strain AHP-3 (open circles) and its *gnd* mutant APG-4 (black circles) in shake flask cultivation. The results represent mean values from five independent cultures. Individual data of biomass and L-lysine concentrations did not deviate from the mean by more than 3%.

Fig. 2. In vivo flux distribution in central metabolism of strains AHP-3 (values on the left of thick arrows) and APG-4 (values on the right of thick arrows) during L-lysine production in batch culture. The exchange coefficients in reversible reactions are given in italics. All fluxes are given relative to moles of glucose carbon (8.3 mmol) consumed though the culture. Abbreviations: G6P, glucose 6-phosphate; F6P, fructose 6-phosphate; P5P, pentose 5-phosphate pool; E4P, erythrose 4-phosphate; S7P, sedoheptulose 7-phosphate; G3P, glyceraldehyde 3-phosphate; DHAP, dihydroxyacetone phosphate; Pyr, pyruvate; AcCoA, acetyl coenzyme A; Cit, citrate; α-KG, α-ketoglutarate; OAA, oxaloacetate; PDC, Δ^1-piperidine 2,3-dicarboxylate.

Fig. A1. Metabolic model and metabolite balance used for in vivo flux determination in strains AHP-3 and APG-4. For reversible reactions, the directions of the net fluxes are indicated by arrows next to the corresponding fluxes (v_5, v_6, v_{11}, v_{12}, v_{13}, v_{14}, v_{15}, v_{16}, v_{17}, v_{19}, v_{29}, and v_{30}). Abbreviations, see Fig. 2.

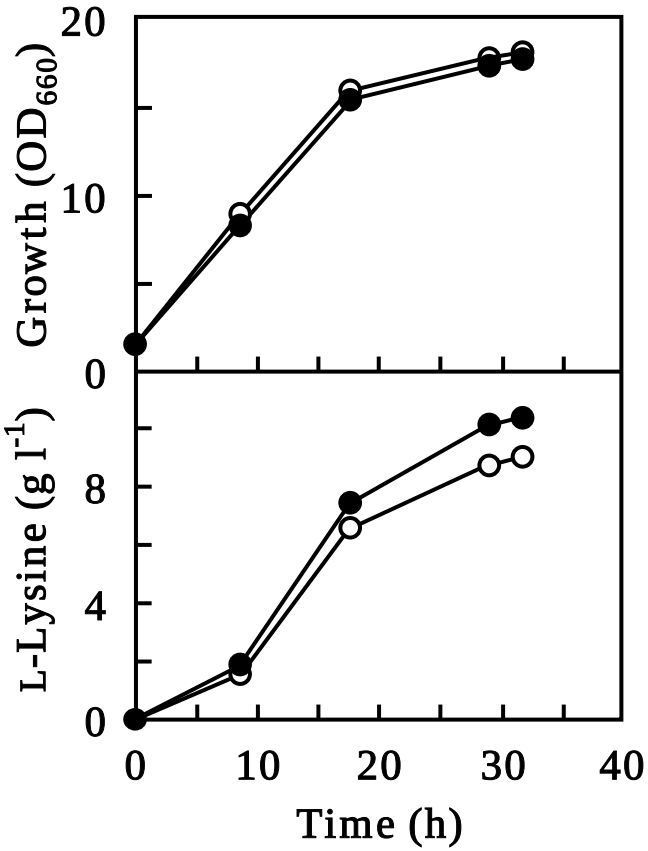
20
10
0
Growth (OD660)
8
4
0
L-Lysine (g l-1)
0
10
20
30
40
Time (h)

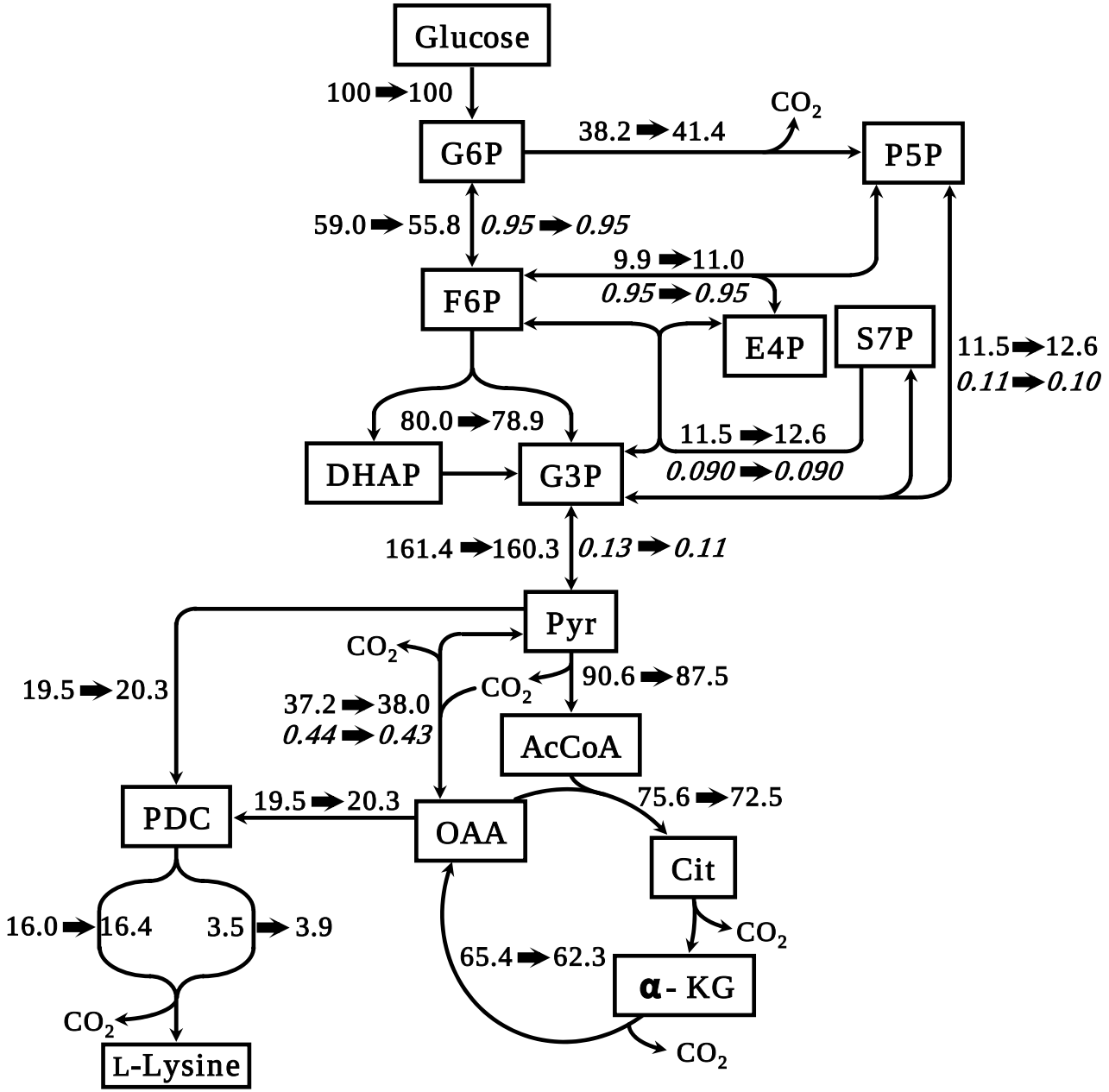
Glucose
100 → 100
G6P
38.2 → 41.4
CO2
P5P
59.0 → 55.8
0.95 → 0.95
9.9 → 11.0
0.95 → 0.95
F6P
E4P
S7P
11.5 → 12.6
0.11 → 0.10
80.0 → 78.9
11.5 → 12.6
0.090 → 0.090
DHAP
G3P
161.4 → 160.3
0.13 → 0.11
Pyr
CO2
19.5 → 20.3
CO2
90.6 → 87.5
37.2 → 38.0
0.44 → 0.43
AcCoA
PDC
19.5 → 20.3
OAA
75.6 → 72.5
Cit
16.0 → 16.4
3.5 → 3.9
CO2
65.4 → 62.3
α - KG
CO2
CO2
L-Lysine

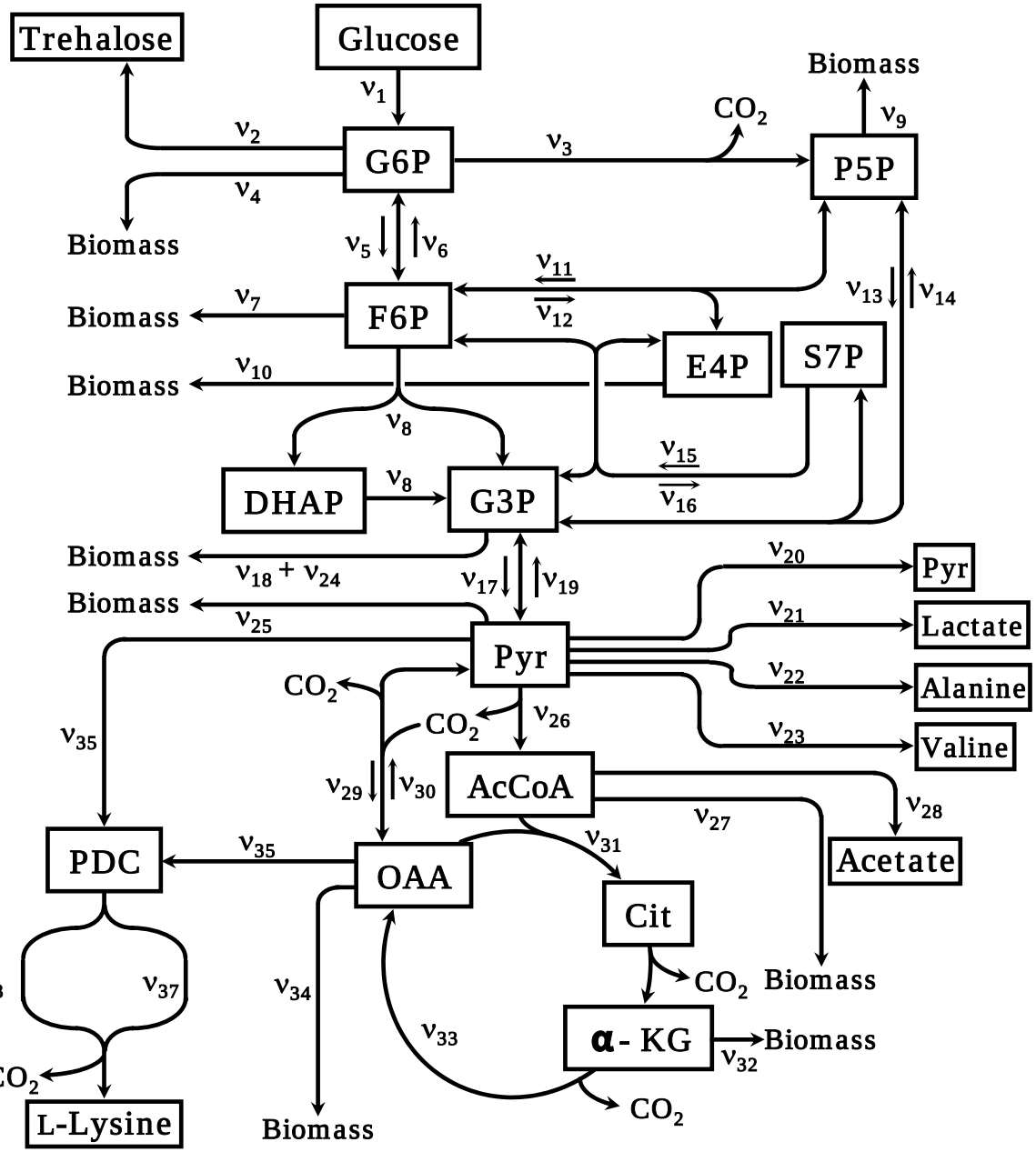
Trehalose
Glucose
Biomass
ν_1
ν_2
CO_2
ν_9
G6P
ν_3
P5P
ν_4
Biomass
ν_5
ν_6
ν_{11}
ν_{13}
ν_{14}
ν_7
ν_{12}
Biomass
F6P
E4P
S7P
ν_{10}
Biomass
ν_8
ν_{15}
DHAP
ν_8
G3P
ν_{16}
Biomass
$\nu_{18} + \nu_{24}$
ν_{17}
ν_{19}
ν_{20}
Pyr
Biomass
ν_{25}
ν_{21}
Lactate
Pyr
ν_{22}
Alanine
CO_2
CO_2
ν_{26}
ν_{23}
Valine
ν_{35}
ν_{29}
ν_{30}
AcCoA
ν_{28}
ν_{27}
ν_{35}
ν_{31}
PDC
OAA
Acetate
Cit
ν_{34}
CO_2
Biomass
ν_{33}
ν_{37}
α- KG
Biomass
ν_{32}
CO_2
CO_2
L-Lysine
Biomass